

A Single Amino Acid Alteration in the Human Parainfluenza Virus Type 3 Hemagglutinin-Neuraminidase Glycoprotein Confers Resistance to the Inhibitory Effects of Zanamivir on Receptor Binding and Neuraminidase Activity

MATTHEW T. MURRELL, MATTEO POROTTO, OLGA GREENGARD,
NATALIA POLTORATSKAIA, AND ANNE MOSCONA*

Department of Pediatrics, Mount Sinai School of Medicine, New York, New York 10029

Received 29 January 2001/Accepted 18 April 2001

Entry and fusion of human parainfluenza virus type 3 (HPF3) requires interaction of the viral hemagglutinin-neuraminidase (HN) glycoprotein with its sialic acid receptor. 4-Guanidino-2,4-dideoxy-2,3-dehydro-*N*-acetylneuraminic acid (4-GU-DANA; zanamivir), a sialic acid transition-state analog designed to fit the influenza virus neuraminidase catalytic site, possesses antiviral activity at nanomolar concentrations in vitro. We have shown previously that 4-GU-DANA also inhibits both HN-mediated binding of HPF3 to host cell receptors and HN's neuraminidase activity. In the present study, a 4-GU-DANA-resistant HPF3 virus variant (ZM1) was generated by serial passage in the presence of 4-GU-DANA. ZM1 exhibited a markedly fusogenic plaque morphology and harbored two HN gene mutations resulting in two amino acid alterations, T193I and I567V. Another HPF3 variant studied in parallel, C-0, shared an alteration at T193 and exhibited similar plaque morphology but was not resistant to 4-GU-DANA. Neuraminidase assays revealed a 15-fold reduction in 4-GU-DANA sensitivity for ZM1 relative to the wild type (WT) and C-0. The ability of ZM1 to bind sialic acid receptors was inhibited 10-fold less than for both WT and C-0 in the presence of 1 mM 4-GU-DANA. ZM1 also retained infectivity at 15-fold-higher concentrations of 4-GU-DANA than WT and C-0. A single amino acid alteration at HN residue 567 confers these 4-GU-DANA-resistant properties. An understanding of ZM1 and other escape variants provides insight into the effects of this small molecule on HN function as well as the role of the HN glycoprotein in HPF3 pathogenesis.

The *Paramyxoviridae* family is comprised of several important agents of human pathology, including measles, mumps, respiratory syncytial, and human parainfluenza viruses. Human parainfluenza virus type 3 (HPF3) is the second leading cause of infant and childhood respiratory disease, including croup, pneumonia, and bronchiolitis. The hallmark cytopathic effect of acute infection with HPF3 in vitro is extensive cell fusion resulting in syncytium formation. For fusion to occur, both interaction of the viral hemagglutinin-neuraminidase (HN) glycoprotein with its sialic acid receptor and presence of the viral fusion (F) glycoprotein are required.

Obvious similarities exist between HPF3 and influenza virus: attachment to host cell surfaces via a sialic acid receptor determinant, and fusion with host cell lipid bilayers (cell surface fusion at neutral pH for HPF3 and low-pH-induced fusion following endocytosis in the case of influenza virus). Both viruses utilize neuraminidase-dependent release of virus from infected cell surfaces. In addition to these parallels in biological strategies, influenza virus neuraminidase (NA) and paramyxovirus HN glycoproteins share structural similarities: both influenza virus NA (1, 4, 37–39) and paramyxovirus HN (5, 6, 17) fold into a propeller-like configuration comprised of

six four-stranded antiparallel β strands arranged about a central cavity.

The study of the neuraminidase inhibitor class of anti-influenza virus compounds began in the early 1970's: 2-deoxy-2,3-dehydro-*N*-acetylneuraminic acid (DANA) (24) and 2-deoxy-2,3-dehydro-*N*-trifluoroacetylneuraminic acid (FANA) (26, 27) were first identified as inhibitors of influenza virus NA in vitro. Recently, more potent and specific inhibitors of influenza virus NA have been developed with the aid of crystallographic data. 4-Guanidino-2,4-dideoxy-2,3-dehydro-*N*-acetylneuraminic acid (4-GU-DANA; zanamivir) is one of these recent additions to the anti-influenza virus armamentarium. 4-GU-DANA, a sialic acid transition-state analog rationally designed against the influenza virus NA glycoprotein, acts as a selective inhibitor of influenza virus A and B NA activity at nanomolar concentrations in vitro and in vivo (40) and is clinically effective (13).

Given the functional and structural similarities of influenza virus and HPF3 and the known potency of 4-GU-DANA for influenza virus NA, it seemed reasonable that this compound might prove efficacious against the neuraminidase of HPF3 HN. Initial observations on Newcastle disease virus (NDV), another member of the *Paramyxovirinae* subfamily, indicated that both DANA and FANA could inhibit NDV neuraminidase activity (24, 26, 27). Moreover, Meindl et al. found that FANA was able to inhibit hemagglutination by NDV, which suggested that the compound could interfere with HN-receptor interactions (24). However, Palese et al. found that FANA did not inhibit attachment of NDV to chicken embryo fibro-

* Corresponding author. Mailing address: Department of Pediatrics, Mount Sinai School of Medicine, 1 Gustave L. Levy Place, New York, NY 10029. Phone: (212) 241-6930. Fax: (212) 426-4813. E-mail: Anne.moscona@mssm.edu.

blasts and concluded that the inhibition of parainfluenza virus plaque formation was via neuraminidase inhibition (27).

The impetus for the present study was provided by data obtained by Levin Perlman et al. that established the ability of DANA to inhibit, at millimolar concentrations, not only the neuraminidase activity but also the receptor interaction of HPF3 HN (18). In plaque assays, the presence of DANA during the adsorption period resulted in a reduction of plaque numbers. Since neuraminidase activity has not been shown to be requisite for viral entry, these plaque reduction data suggested that the inhibitory mechanism involved disruption of HN-receptor interaction and not neuraminidase inhibition. Similar results were subsequently obtained with 4-GU-DANA: Greengard et al. showed that HPF3 neuraminidase activity, hemadsorption (HAD), and fusion of persistently infected cells with uninfected cells were inhibited by 4-GU-DANA (9). We therefore reasoned that selection of resistant HPF3 variants using 4-GU-DANA could provide tools for understanding the multiple roles of HN during HPF3 infection.

The generation of influenza virus variants resistant to 4-GU-DANA has been well documented and has yielded insight into the molecular basis of resistance as well as the functional importance of several NA catalytic site residues (2, 3, 10–12, 20–22). Our initial HPF3 4-GU-DANA studies, coupled with the existence of the informative influenza virus variants generated *in vitro*, led us to postulate that the generation of HPF3 escape variants by using 4-GU-DANA would prove informative regarding the mechanism of inhibition of the dual functions of HN by 4-GU-DANA. Moreover, these variants promised to be ideal tools for gaining a greater understanding of the role of HN in HPF3 pathogenesis. In this study, we present data characterizing the first paramyxovirus variant selected with 4-GU-DANA and present hypotheses regarding the mechanism of resistance as well as the future prospects of this class of inhibitors for use against paramyxovirus infections.

MATERIALS AND METHODS

Cells and virus. CV-1 (African green monkey kidney) cells were grown in Eagle's minimal essential medium (Mediatech Cellgro) supplemented with L-glutamine, antibiotics, and 10% fetal bovine serum. HPF3 wild-type (WT) stock was prepared by infecting CV-1 cell monolayers at a multiplicity of infection (MOI) of 0.1. Viral supernatant fluid was collected, spun at 3,000 rpm (2,060 × g) in a Beckman GS-6R centrifuge equipped with a Beckman G.H. 3.8 rotor for 5 min to clear cellular debris and frozen in aliquots at –80°C. Variant virus stocks were made in CV-1 cell monolayers from virus that was plaque purified three times. Viral titers were determined by a standard plaque assay in CV-1 cells. All infections were performed on CV-1 cell monolayers in serum-free medium. Following a 90-min adsorption period during which the cell monolayers were gently rocked at 15-min intervals, the inoculum was aspirated and replaced with fresh serum-free medium. All cell photographs were taken with a 35-mm camera (Nikon N2000) attached to an inverted phase-contrast microscope (Nikon TMS) using the 10× objective.

Sialic acid transition-state analog. 4-GU-DANA, a transition-state analog of sialic acid rationally designed against the influenza virus A and B NA (40), was prepared as a 50 mM stock solution in serum-free medium and stored at –20°C. 4-GU-DANA used in this study was a generous gift from Glaxo Wellcome Research and Development Ltd. (Stevenage, United Kingdom).

RBC. Human red blood cells (RBC) were obtained from whole-blood samples drawn into EDTA vacuum tubes. Samples were washed with cold phosphate-buffered saline (PBS; pH 7.4) and centrifuged for 5 minutes at 3,000 rpm (2,060 × g) (Beckman GS-6R centrifuge with a Beckman G.H. 3.8 rotor). RBC were then resuspended in serum-free medium as a 10% RBC stock stored at 4°C. The cells were used within 5 days of collection.

Generation of variant virus by using 4-GU-DANA. HPF3 WT stock was propagated in CV-1 cells in the presence of alternating concentrations of 4-GU-DANA. An initial, selective concentration of 3 mM 4-GU-DANA was used in combination with a lower, permissive concentration of 0.3 mM 4-GU-DANA. Virus-containing supernatant fluid was collected after 24 to 48 h of infection and used to inoculate new CV-1 cell monolayers. Following each 0.3 mM passage, virus-containing supernatant fluid was also collected and diluted for use in a plaque assay assessing the effect of 4-GU-DANA on infectivity and plaque size. After four passages at alternating concentrations, phenotypically variant plaques were identified, picked, and used to infect new CV-1 cell monolayers in 3 mM 4-GU-DANA. The resulting isolates were plaque purified in the presence of 12.5 mM 4-GU-DANA and subsequently plaque purified three times in the absence of drug to ensure stability of the variants. One isolate (designated ZM1) was used as the source of variant stock in the experiments presented here.

RNA isolation and sequence analysis of HN and F genes. Total RNA was isolated from CV-1 cell monolayers in 175-cm² flasks infected with WT, C-0, or ZM1 at an MOI of 5. After 24 to 48 h of incubation, the cell monolayers were lysed directly with TRIzol reagent (Life Technologies, Inc.), homogenized by pipetting, and incubated for 5 min at room temperature. Chloroform was added in a 1:7 ratio to the TRIzol suspension, which was then vortexed and incubated on ice for 5 to 10 min. The samples were then centrifuged at 14,000 rpm for 15 min at room temperature in a tabletop microcentrifuge (Microspin 24S; Sorvall Instruments, Du Pont), after which the RNA-containing upper aqueous phase was collected. The aqueous phase was then precipitated with isopropyl alcohol at a 1:2 ratio with the initial TRIzol volume used, vortexed, and incubated at –20°C for 30 min. Following a 10-min centrifugation at 14,000 rpm at room temperature in a tabletop microcentrifuge, the RNA pellet was washed with 80% ethanol and air dried. The pellet was resuspended in formamide at 65°C with agitation, and the $A_{260/280}$ ratio was determined in a spectrophotometer (Ultrospec 2000, Pharmacia Biotech). RNA isolated in this manner was subjected to reverse transcription using F (5' GGGGAAGCTTATAATTTTAAATATCTAATG 3')- and HN (5' GGGGGATCCATATTTCTCTTTTATCTATTGTCTGATTGCT 3')-specific primers complementary to the 3' termini (underlined). The reaction products were then used as template cDNAs for PCR amplification using 5'-terminus-specific primers (F, 5' CCCGGATCCAGGACAAAAGAAGTC 3'; HN, 5' CCCGAATTCAGGAGTAAAGTTACGC 3'). Sequencing primers were designed against the HN and F WT sequences at approximately 200-bp intervals (25). Sequencing reactions were performed by the Biotechnology Center of Utah State University, Logan. Sequence analysis was carried out on the DNA products of two separate isolations and performed twice on all samples to confirm sequence alterations.

Viral growth curves. The release of virus at various times postinfection was assessed by plaque assay of viral supernatant fluid. Duplicate CV-1 cell monolayers grown in 60-mm dishes were infected with WT, C-0, and ZM1 at an MOI of 5. Following a 90-min adsorption period, the inoculum was aspirated and replaced with serum-free medium. At 3, 6, 9, 13, 21, and 25 h postinfection, duplicate 100- μ l aliquots were collected and used in a plaque assay to determine the viral titer. Viral titer values obtained from these samples were averaged and plotted as PFU per milliliter at each time point.

HAD assays. CV-1 cell monolayers (24-well plates, 4 × 10⁵ cells/well) were infected with WT, C-0, or ZM1 at an MOI of 5. Following aspiration of the inoculum 90 min later, the medium was replaced with 1 ml of serum-free medium containing 0.1 U of *Clostridium perfringens* neuraminidase (type X; Sigma Scientific N-2133), and the cells were incubated at 37°C for 18 h. The medium was then aspirated and replaced with 200 μ l of 0.5% RBC in serum-free medium containing 0, 3, 6, or 12.5 mM 4-GU-DANA. The cell monolayers were leveled with a bubble level and placed at 4°C for 2 h. The wells were then washed four times with cold serum-free medium and photographed. Quantification of the bound RBC was achieved by RBC lysis with 250 μ l of 50 mM NH₄Cl, and the absorbance was read at 540 nm on an enzyme-linked immunosorbent assay reader (Kinetics Reader model EL312e; BIO-TEK Instruments, Winooski, Vt.).

Plaque assays and plaque reduction assays. The effect of 4-GU-DANA on plaque number was assessed by a plaque reduction test performed as described elsewhere (18). Briefly, CV-1 cell monolayers were inoculated with 100 to 200 PFU of WT, C-0, or ZM1 in the presence of various 4-GU-DANA concentrations. After 90 min, 2× minimal essential medium containing 10% fetal bovine serum was mixed with 1% agarose and added to the dishes. This agarose overlay contained no 4-GU-DANA. The plates were then inverted and incubated at 37°C for 24 h. After removal of the agarose overlay, the cells were immunostained for plaque detection (18). Plaques in the control (no drug) and experimental wells were counted under a dissecting stereoscope. For experiments presenting plaque area measurements as a function of 4-GU-DANA concentration, plaque diameter was measured at a magnification of ×7 to ×45 under a zoom stereomicro-

scope equipped with a micrometer. Surface area calculations from 20 plaques were used to establish mean plaque areas with deviation.

Neuraminidase assays. Viral preparations were obtained from a 0.1-MOI infection of 20 175-cm² culture flasks of CV-1 cells. Viral supernatant fluid was collected after 24 to 48 h and centrifuged at 3,000 rpm (2,060 × g) for 5 min in a Beckman GS-6R centrifuge equipped with a Beckman G.H. 3.8 rotor to clear cell debris. The supernatant fluid was transferred to a new tube and centrifuged at 25,000 rpm (120,000 × g) for 130 min at 4°C in a Beckman Optima L-70K Ultracentrifuge (Beckman Instruments, Inc.) with an SW28 swing tube rotor. The viral pellet was then resuspended in Tris-EDTA buffer (pH 7.4), loaded onto an 11-ml 7 to 60% sucrose gradient, and spun for 24 h in an SW41-Ti rotor at 35,000 rpm (230,000 × g) at 4°C. The lower half of the sucrose gradient was then collected, diluted with serum-free medium, and spun in an SW28 rotor at 25,000 rpm (110,000 × g) for 130 min. The final pellet was then suspended in 200 to 300 μl of 100 mM malate buffer (pH 4.75). Before use in the neuraminidase assay, the viral preparation was sonicated on ice for 15 s in a 550 Sonic Dismembrator (Fisher Scientific). Total protein concentrations were determined by the Bio-Rad protein assay (Bio-Rad Laboratories, Hercules, Calif.). The fluorimetric assay of neuraminidase in sonicated HPF3 preparations was based on the methods of Warner and O'Brien (41) and Potier et al. (31). Reaction mixtures, containing 100 mM malate buffer (pH 4.75) and the indicated concentrations of MUNANA (4-methylumbelliferyl- α -D-N-acetylneuraminic acid) in a total volume of 25 μl, were incubated at 37°C for 15 to 20 min. To determine the rate of product formation, samples were taken at four to five time points, mixed with 100 mM ethylenediamine, and read in a Sequoia-Turner fluorimeter at 365-nm excitation wavelength and 450-nm emission wavelength. The amount of reaction product denoted by these readings was determined from fluorescence versus concentration curves determined with commercially obtained 4-methylumbelliferone. Fluorescence resulting from the spontaneous hydrolysis of substrate, corrected for as described by Potier et al. (31), was always less than 25% of the total. Enzyme activity is expressed in nanomoles of product formed per minute per milligram of total protein.

Western blot analysis of viral preparations was performed by analyzing equal amounts of total protein on a sodium dodecyl sulfate-11% polyacrylamide gel. Aliquots containing 2.5 and 5 μg of total protein were resolved in parallel with identical concentrations of a standard WT HPF3 preparation. The gel was transferred to a Hybond-P polyvinylidene difluoride membrane (Amersham Life Science, Buckinghamshire, United Kingdom) by electroblotting in a transblot apparatus (Hoefer Scientific Instruments) for 2 h at 4°C at 100 V (Bio-Rad Tris-glycine buffer [25 mM Tris, 192 mM glycine {pH 8.3}]). The membranes were then blocked with a solution of 10% dry milk in PBS with 0.05% Tween 20 (in PBST) for 1 h, rinsed once with PBST, and immunoblotted with polyclonal guinea pig anti-HPF3 serum (BioWhittaker, Walkersville, Md.), 1:1,000 in 1% bovine serum albumin in PBST, for 1 h at room temperature. Membranes were rinsed three times with PBST and incubated with peroxidase-conjugated protein A (5 μg/μl; 1:100,000) (ImmunoPure Recomb Protein A; Pierce, Rockford, Ill.) for 1 h at room temperature. Films were developed using Supersignal West Dura extended-duration substrate (Pierce) according to the manufacturer's instructions.

RESULTS

Variant virus isolation using 4-GU-DANA. WT HPF3 was passaged in CV-1 cell monolayers in the presence of alternating 4-GU-DANA concentrations. Figure 1 outlines the selection strategy. A high 4-GU-DANA concentration (3 mM) was used to select for resistant viruses, while a lower drug concentration (0.3 mM) was chosen to permit amplification of any viruses surviving the higher, selection concentration. WT HPF3 stock at an MOI of 0.1 was used to infect CV-1 cell monolayers in the presence of 3 mM 4-GU-DANA (passage 1). Supernatant fluid was collected 48 h later and used to infect new CV-1 cell monolayers in the presence of 0.3 mM 4-GU-DANA (passage 2). Supernatant fluid again was collected at 48 h and used for passage into CV-1 cell monolayers in the presence of 3 mM 4-GU-DANA (passage 3). Supernatant fluid from the 3 mM 4-GU-DANA passage was used for infecting cells at 0.3 mM 4-GU-DANA (passage 4). Viruses emerging from this passage exhibited large, sprawling areas of complete fusion (Fig. 2, ZM1). Supernatant fluid from passage 4 was

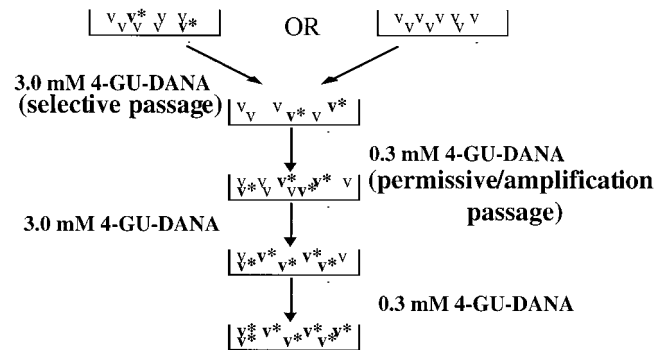


FIG. 1. Selection scheme for isolation of a variant HPF3 virus by using 4-GU-DANA. WT stock was propagated in CV-1 cells at an MOI of 0.1 in the presence of alternating 4-GU-DANA concentrations (0.3 and 3.0 mM). Variants are indicated with asterisks. Two alternatives for the emergence of variants are presented: variants preexisting at low number in the parental stock and variants arising during the selection process. Morphologic variants identified in passage 4 (0.3 mM) were plaqued twice in the presence of 12.5 mM 4-GU-DANA and then subjected to three rounds of plaque purification in the absence of 4-GU-DANA.

used to infect cells in the presence of 3 mM 4-GU-DANA; plaques emerging on these cell monolayers were picked and plaqued twice in 12.5-mM 4-GU-DANA. Following these final selection passages, the variants were plaque purified three times in the absence of 4-GU-DANA. The experiments presented here were conducted with a large-plaque variant designated ZM1.

Comparison of WT and variant plaque morphologies. The 4-GU-DANA-resistant variant virus (ZM1) was identified and isolated based on its plaque morphology being distinct from that of the parental HPF3. Interestingly, a fusogenic HPF3 variant (C-0) that we previously isolated by selection with exogenous neuraminidase treatment exhibits a plaque phenotype nearly identical to that of ZM1 (25). A single mutation in HN (T193A) resulted in the C-0 variant's fusogenic plaque phenotype and increased receptor-binding affinity. To obtain a comparison of plaque development, CV-1 cell monolayers (5×10^5 cells) were infected with 100 PFU of WT, C-0, or ZM1 virus. Figure 2 shows that WT infection resulted in the production of stellate fusion areas interspersed with intact cells characteristic of WT HPF3. Both the C-0 and ZM1 variants, however, produced larger fused areas devoid of intact, unfused cells. Moreover, these plaques emerged earlier than their WT counterparts. These shared morphological characteristics provided an initial suggestion of relatedness between the ZM1 and C-0 variants.

Sequence analysis of ZM1 variant HN and F genes. An understanding of the ZM1 variant necessitates a correlation of structural alterations with functional and phenotypic alterations. Total RNA from infected CV-1 cells was used as a template for reverse transcription and PCR amplification of the F and HN genes. Sequence alignment of ZM1 and WT F amino acid sequences revealed no mutations. Alignment of the HN sequences revealed two mutations in the ZM1 variant that result in T193I (cytosine-to-thymine nucleotide alteration at base 2564) and I567V (adenine-to-guanine nucleotide alteration at base 3685) amino acid alterations (Table 1; Fig. 3).

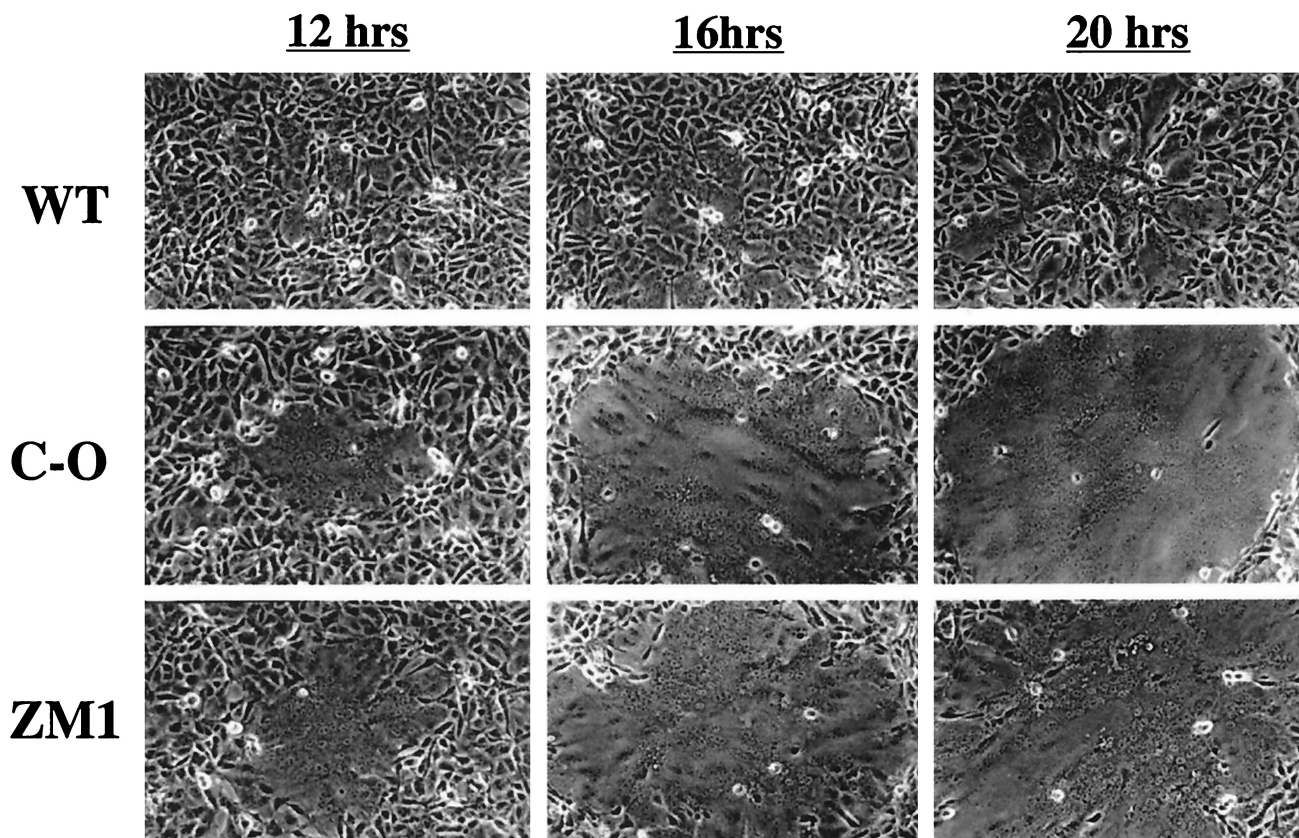


FIG. 2. Plaque morphologies of WT, C-0, and ZM1. CV-1 cells (5×10^5) were infected with 100 PFU of WT, C-0, or ZM1 and overlaid with 0.5% agarose following a 90-min adsorption period. Photographs were taken at 12, 16, and 20 h postinfection.

The base alteration at position 2564 introduced a novel *Eco*RI site, thus facilitating identification of the variant HN. Importantly, the C-0 variant shared with ZM1 an alteration at residue 193; this variant possessed a T193A alteration (25). In addition to the plaque morphology alteration, C-0 also possessed increased HN receptor binding affinity, thus implicating residue 193 in receptor binding (25). As a means of attributing viral functions to particular structural alterations, and more specifically to separate the contribution of the residue 193 alteration from that of the residue 567 alteration, C-0 was studied in parallel with both WT and ZM1 throughout this study.

Comparison of HPF3 WT, C-0, and ZM1 growth kinetics. Although the selective pressure exerted by 4-GU-DANA should be limited to the mutated HN molecule and its binding and enzymatic functions, other reasons for the altered behavior of the ZM1 variant must be excluded. One such reason may

be an alteration in the kinetics of growth, as measured by virion release from infected cell monolayers. Figure 4 presents a comparison of virion release following infection of CV-1 cell monolayers with WT, C-0, or ZM1 at an MOI of 5. These conditions were chosen so that every cell would be infected at the time of the initial infection and growth parameters would not be influenced by fusogenicity. Earlier work from our laboratory indicated that C-0 and WT growth characteristics were identical, as assessed by the viral protein production rate in metabolically labeled infected cell monolayers and the release of radiolabeled virions (25). WT and ZM1 were indistinguishable throughout the course of the experiment presented in Fig. 4, indicating that viral growth kinetics do not explain the behavioral differences exhibited between these viruses.

Effect of 4-GU-DANA on neuraminidase activity of WT and variants. A fluorimetric neuraminidase assay was adapted for use with HPF3 (9). Viral preparations were incubated at 37°C with the fluorogenic substrate MUNANA at the pH optimum (4.7) of the viral neuraminidase. At each of two different enzyme concentrations, samples were collected at four time points during the 15-min incubation and assayed to ensure that the rate of catalysis was constant and proportional to the amount of enzyme in the system.

Results obtained from assays of separate viral preparations of each virus performed in triplicate revealed no significant differences in absolute neuraminidase activity among WT, C-0, and ZM1 (data not shown). However, clear differences

TABLE 1. HPF3 variant amino acid alterations

HPF3 variant	Alteration	Phenotype
C-0	T193A	Enhanced receptor binding and fusion promotion
ZM1	T193I I567V	Enhanced fusion promotion 4-GU-DANA-resistant plaque formation; receptor-binding and neuraminidase activities

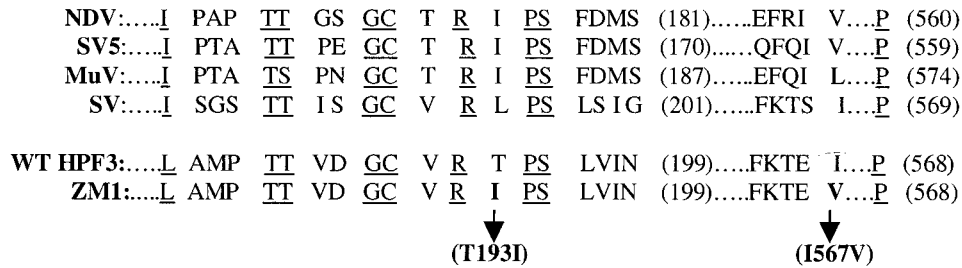


FIG. 3. Partial paramyxovirus HN amino acid alignment. The two ZM1 alterations are indicated in their HN regional context, aligned with corresponding residues of related paramyxovirus HN sequences. Both amino acid mutations lie adjacent to highly conserved residues. Underlined residues represent conserved amino acids; bold residues indicate HPF3 variant amino acid alterations from WT stock.

emerged upon addition of 4-GU-DANA to the assay system; variant ZM1 is highly resistant to the neuraminidase inhibitory effect of 4-GU-DANA. Figure 5 depicts the inhibition of neuraminidase activity, presented as a function of the 4-GU-DANA concentration. Consistent with previous studies on the inhibition of WT by 4-GU-DANA in which the 50% inhibitory concentration was identified as 0.8 mM (9), 50% inhibition for both WT and C-0 neuraminidase was achieved at 0.5 mM. The 50% inhibition level for ZM1 was between 5 and 10 mM 4-GU-DANA, indicating a 10 to 20-fold increase in resistance of variant ZM1 over both WT and C-0. At the lowest 4-GU-DANA concentration assayed, both WT and C-0 neuraminidases were inhibited by more than 50%, while activity of ZM1 was reduced by only 9%. In the presence of 5 mM 4-GU-DANA, both WT and C-0 neuraminidases were nearly completely inhibited (92.4 and 95.7% inhibition, respectively), whereas ZM1 activity levels were reduced by less than half (43.5% inhibition). Inhibition increased only slightly for WT (94% inhibition) and C-0 (98.2% inhibition) at 10 mM 4-GU-DANA. These results indicate that an alteration at HN residue 193 shared by C-0 and ZM1 does not confer the 4-GU-DANA resistance of the viral neuraminidase and that this resistance was conferred by the alteration at residue 567. It is also possible that cooperativity between the two amino acid alterations

(residues 193 and 567) is required for the ZM1 neuraminidase resistance evident in this study.

Effect of 4-GU-DANA on receptor binding. 4-GU-DANA has been shown to inhibit the interaction of HPF3 HN with its receptor (9). The ability of WT, C-0, and ZM1 to bind sialic acid receptors was assessed by a quantitative HAD assay. Infected cell monolayers were treated with 0.1 U of *C. perfringens* neuraminidase after the virus adsorption period to prevent fusion throughout the monolayer; prior to addition of RBC, the cells were washed thoroughly to remove the exogenous neuraminidase. RBC, used as receptor donors, were incubated with infected cell monolayers at 4°C, a temperature that permits the receptor-binding but not the receptor-destroying (neuraminidase) activity of HN. Bound RBC were then lysed, and the absorbance values of the lysates provided a quantitative measure of HN receptor binding. Figure 6A presents the percent inhibition of HAD for cell monolayers infected with WT, C-0, or ZM1 in the presence of various 4-GU-DANA concentrations. Figure 6B shows micrographs of these infected cell monolayers with bound RBC along with percent inhibition for each. In the absence of 4-GU-DANA, all three viruses exhibited similar RBC binding. However, upon addition of 1

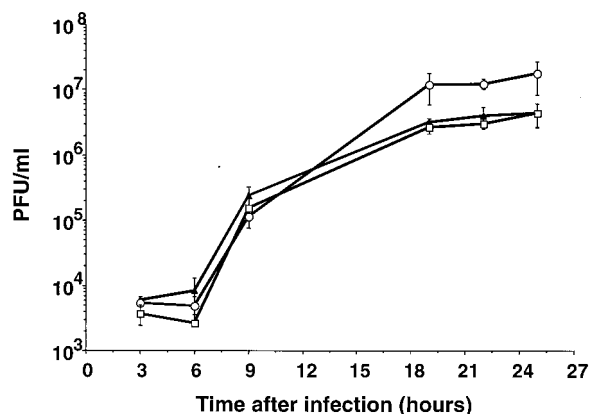


FIG. 4. Kinetics of virion release from infected cells into supernatant fluid. Duplicate CV-1 cell monolayers were infected at an MOI of 5 with WT (filled triangles), C-0 (open circles) or ZM1 (open squares). The number of infectious particles released at each time point was determined by plaque assay.

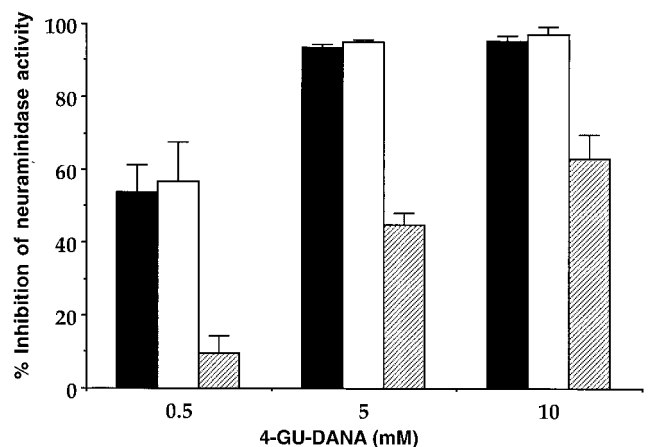


FIG. 5. Inhibition of neuraminidase activity of WT (filled bars), C-0 (open bars), and ZM1 (striped bars) by 4-GU-DANA. Viral preparations were assayed using a substrate concentration of 20 mM in the absence and presence of 4-GU-DANA. Bars indicate the percent inhibition of neuraminidase activity (nanomoles per minute per milligram of protein) as a function of millimolar 4-GU-DANA and are the means (with standard deviations) of at least three experiments.

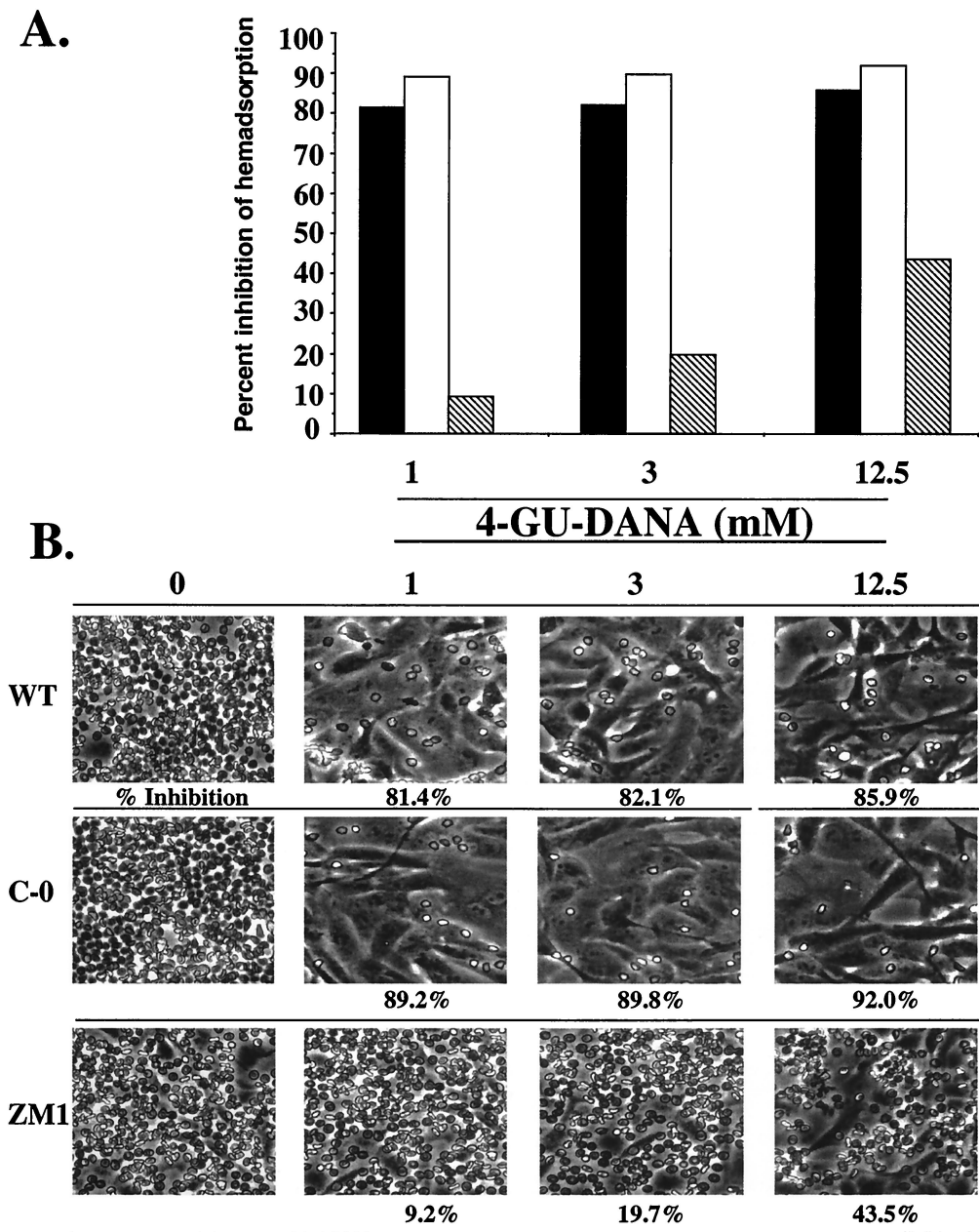


FIG. 6. Inhibition of HAD for WT-, C-0-, and ZM1-infected cells by 4-GU-DANA. CV-1 cell monolayers were infected with the indicated virus at an MOI of 5; following a 90-min adsorption period, the cell monolayers were washed and treated with 0.1 U of *C. perfringens* neuraminidase to prevent fusion of the infected cell monolayers. HAD was assayed at 4°C at 18 h postinfection. Percent inhibition of HAD (expressed relative to RBC binding in the absence of 4-GU-DANA) was determined by quantitating bound RBC. (A) Percent inhibition of HAD for WT (filled bars), C-0 (open bars), and ZM1 (striped bars). (B) Micrographs of WT-, C-0-, and ZM1-infected cell monolayers indicating the amount of HAD at each 4-GU-DANA concentration. Percent inhibition, given beneath each panel, represents the results of two separate experiments each performed in triplicate culture wells.

mM 4-GU-DANA, significant differences in the receptor-binding ability of the viruses were evident. ZM1 was resistant to the binding-inhibitory effect of 4-GU-DANA, as evidenced by approximately 10-fold less inhibition of receptor binding than both WT and C-0 at 1 mM 4-GU-DANA (9.2, 81.4, and 89.2% inhibition, respectively). Increasing the 4-GU-DANA concentration had little additional inhibitory effect on WT and C-0 HAD (3 and 12.5 mM panels), suggesting near-maximal inhi-

tion at 1 mM. In contrast, the inhibition of ZM1 HAD increased as the 4-GU-DANA concentration was raised, with only 43.5% inhibition at 12.5 mM 4-GU-DANA. As was evident for neuraminidase activity, the sensitivity of C-0 to 4-GU-DANA's effect on HAD was indistinguishable from that of WT, indicating that the alteration at HN amino acid 567, and not that at 193, conferred sialic acid receptor binding resistance to 4-GU-DANA.

Effect of 4-GU-DANA on infectivity and plaque enlargement.

The ability of 4-GU-DANA to inhibit the formation and the enlargement of plaques was assessed in plaque reduction assays. To assess infectivity, CV-1 cell monolayers (5×10^5 cells) were infected with 200 to 300 virus particles in the presence of various 4-GU-DANA concentrations. After the 90-min adsorption period, the monolayers were overlaid with agarose containing 4-GU-DANA. Following immunostaining of the cell monolayers 24 h later, the plaques were counted. Figure 7A, which depicts plaque numbers expressed as percent inhibition of the number formed in the absence of 4-GU-DANA, shows that the presence of 1 mM 4-GU-DANA reduced both WT and C-0 plaque numbers to less than 10% of control values (WT, 94.8 and 98.7% inhibition; C-0, 95.9 and 96.6% inhibition). ZM1, however, was unaffected by 1 mM 4-GU-DANA, with plaque numbers equivalent to or slightly higher than control numbers (5.7 and 9.6% greater than control values). Consistent with these data, 15 mM 4-GU-DANA completely inhibited plaque formation by both WT and C-0 while causing only 42.4 and 28.1% inhibition of ZM1 plaque formation.

The inhibition of plaque enlargement by 4-GU-DANA is illustrated in Fig. 7B, which shows that ZM1 was resistant to the effects of 4-GU-DANA on plaque enlargement. For HPF3, plaque enlargement occurs by fusion of an infected cell with an adjacent uninfected cell and reflects HN-receptor interaction without release of virus into the supernatant fluid. In the absence of the inhibitor, stained plaques were visible with the naked eye in the WT, C-0, and ZM1 wells. However, addition of 1 mM 4-GU-DANA resulted in diminution of WT and C-0 plaques. Plaques were visible in these wells only when viewed under a stereoscope, indicating that plaque size was markedly reduced by 4-GU-DANA (stereoscopic view not shown); no WT or C-0 plaques were visible under the stereoscope at 15 mM 4-GU-DANA. In contrast, the ability of ZM1 to produce plaques visible without the stereoscope at 1 mM 4-GU-DANA (Figure 7B) indicates that the inhibitor had no visible effect on plaque enlargement at this concentration. The ability of ZM1 to produce plaques in the presence of 15 mM 4-GU-DANA is shown in the enlargement of the 15 mM well. Under these conditions, minute ZM1 plaques were visible.

To quantify the inhibition of plaque enlargement by 4-GU-DANA, we performed a modification of the plaque assay in which the inhibitor was present only after the 90-min adsorption period. Thus, its effects were limited to the period when binding and entry have occurred and plaques are enlarging by fusion of infected cells with adjacent uninfected cells. Figure 8 shows the average plaque area of 20 plaques from each virus in the absence or presence of 1 mM 4-GU-DANA and demonstrates the resistance of ZM1 to 4-GU-DANA under these conditions. The plaque sizes of both WT and C-0 were each inhibited by 99.9% (from 0.352 to 0.0002 mm² for WT; from 0.615 to 0.0002 mm² for C-0). Photographs taken of representative wells demonstrate this diminution of plaque area to sizes visible only under the stereoscope. Under identical conditions, ZM1 plaque area was inhibited only 30.9% (from 0.598 to 0.413 mm²), and photographs of the stained plaques reveal that they were readily visible without magnification under the stereoscope. Thus, ZM1 was relatively resistant to the inhibition of both plaque number and plaque enlargement produced by 4-GU-DANA.

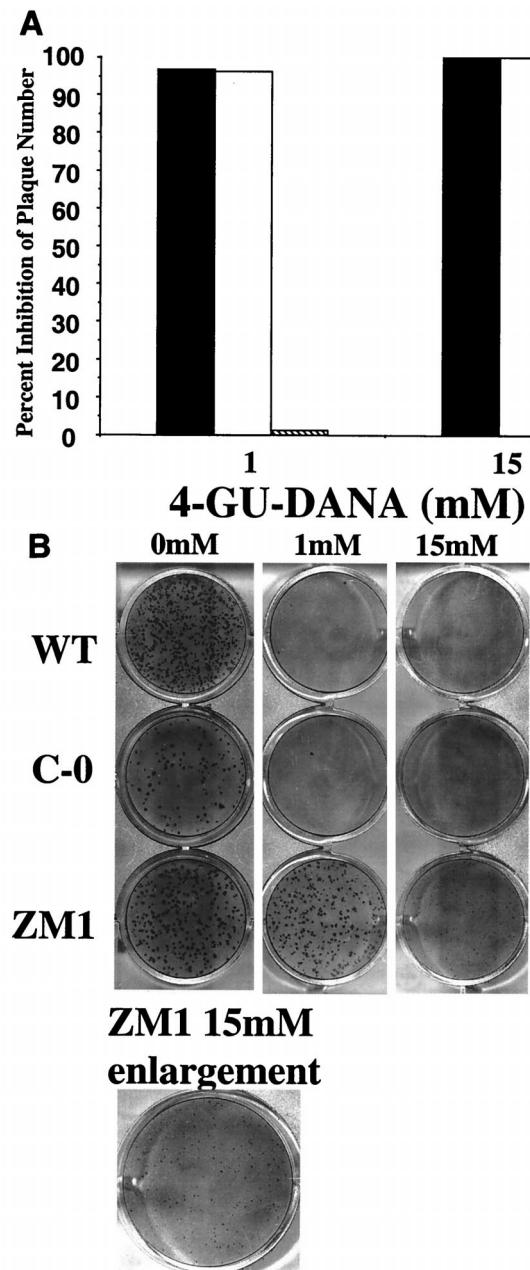


FIG. 7. Reduction of WT, C-0, and ZM1 infectivity by 4-GU-DANA. (A) CV-1 cell monolayers (5×10^5 cells) were infected with 200 to 300 PFU of WT (filled bars), C-0 (open bars), or ZM1 (striped bars) in the presence of the indicated 4-GU-DANA concentration. Plaque numbers are presented as percentage of the number formed in the absence of 4-GU-DANA. Each data bar represents the results from two separate experiments performed in quadruplicate culture wells. The striped bar at 1 mM 4-GU-DANA indicates no inhibition of ZM1 at this inhibitor concentration. (B) Photographs of the plaque reduction assay data presented in panel A. The enlargement of the ZM1 15 mM well shows minute plaques not otherwise visible. Similarly sized plaques were visible in the WT and C-0 1 mM, but not 15 mM, wells (enlargement not shown).

DISCUSSION

In this study, we present the characterization of the first variant paramyxovirus resistant to the sialic acid transition-state analog neuraminidase inhibitor 4-GU-DANA. Variant


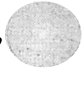
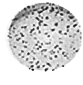



Virus	4-GU-DANA (mM), at 90 min	Plaque Area (mm ²)	% Reduction
WT	0	0.352 +/- 0.006	
	1.0	0.0002 +/- 1.0x10 ⁻⁵	99.9% 
C-0	0	0.615 +/- 0.019	
	1.0	0.0002 +/- 1.0x10 ⁻⁵	99.9% 
ZM1	0	0.598 +/- 0.013	
	1.0	0.413 +/- 0.002	30.9% 

FIG. 8. Inhibition of WT, C-0, and ZM1 plaque enlargement by 4-GU-DANA. Cells (5×10^5) were infected with 300 PFU of WT, C-0, or ZM1 in the absence of 4-GU-DANA. After a 90-min adsorption period, viral supernatant was aspirated and replaced with agarose containing 1 mM 4-GU-DANA. Cell monolayers were fixed and immunostained 18 h later. Plaque area was calculated from diameter measurements taken with a zoom stereomicroscope micrometer. Percent inhibition of plaque enlargement was determined by comparing the mean area (\pm standard deviation) of 20 plaques in control and experimental culture wells.

ZM1, which emerged after passage in CV-1 cells in the presence of 4-GU-DANA, exhibited a markedly fusogenic phenotype and replicated and released viral progeny at 4-GU-DANA concentrations restrictive for WT HPF3 growth. Two amino acid alterations in HN were identified. ZM1 was approximately 15-fold less sensitive to 4-GU-DANA than WT in measures of receptor binding and neuraminidase activity. The variant was also resistant relative to WT in measures of inhibition of infectivity and the ability of plaques to enlarge and spread throughout cell monolayers in the presence of 4-GU-DANA.

Correlation of structural alterations with functional changes elucidates the specific contribution of those protein regions to viral biological activity. Sequence analysis of the ZM1 and WT HN glycoprotein genes revealed two amino acid alterations, T193I and I567V. C-0, a fusogenic variant with enhanced receptor-binding affinity, harbors only a T193A alteration and is not resistant to 4-GU-DANA. We postulate that the T193I alteration imbues the ZM1 variant with enhanced receptor-binding affinity, and thus a markedly fusogenic phenotype similar to that of C-0 (T193A), while the I567V alteration may provide 4-GU-DANA resistance. However, it is possible that the two mutations act cooperatively to produce the 4-GU-DANA-resistant phenotype of ZM1.

Since we detected no differences in the specific activity of neuraminidase between ZM1 and WT that may have accounted for 4-GU-DANA resistance, the I567V alteration in the ZM1 HN may confer multifunctional 4-GU-DANA resistance by reducing the availability of the molecule to the active site(s) rather than by altering the neuraminidase activity. The mutation at residue 567 may impede binding of 4-GU-DANA to the active site(s), either alone or in cooperation with the 193 alteration. The exact contribution of mutations at residue 567 to 4-GU-DANA escape remains to be determined. It is a theoretical possibility that mutations in genes coding for internal virion proteins may contribute to the ZM1 phenotype, although such mutations would not be expected to arise under 4-GU-DANA selection pressure. The success of recovering infectious HPF3 clones from cDNA and thereby generating mutated viruses has provided tools with which to discern the impact of individual mutations on viral phenotypes (7, 14). Construction of such recombinant viruses would provide rigorous proof of the contribution of residue 567 as well as the potential cooperativity of residues 193 and 567 in terms of resistance to 4-GU-DANA's effects on receptor binding, neuraminidase, and infectivity. Expression of singly mutated HN on mammalian cell surfaces will allow us to further explore the individual contributions of the two alterations to receptor binding and neuraminidase activity and to the 4-GU-DANA resistance of these two properties in the ZM1 variant.

It has not escaped our notice that ZM1 HN has been altered such that the amino acids at 193 and 567 are identical to both NDV and simian virus 5 HN. This raises the possibility that if these residues in fact confer 4-GU-DANA resistance to ZM1, WT NDV and simian virus 5 HN may be resistant to the inhibitor; we are currently exploring the sensitivity of these viruses to 4-GU-DANA.

One possible explanation for ZM1's resistance to 4-GU-DANA may be decreased affinity of the HN active site(s) for the inhibitor. No previous studies have implicated residue 567 in either neuraminidase activity or receptor binding, and sequence comparisons of influenza virus NA and paramyxovirus HN (5) and crystallographic evidence from NDV HN (6) suggest that this residue is not within the binding pocket of influenza virus NA or NDV HN. Nevertheless, an alteration at residue 567 confers a striking, multifunctional resistance (resistance to both neuraminidase activity and receptor binding) to 4-GU-DANA in our assays, and determination of this residue's functional contribution to resistance, including expression of singly mutated HN molecules, will expand upon the work presented here.

Although the 4-GU-DANA escape variant that we identified had alterations at both residues 193 and 567, it is possible that resistant variants harboring an alteration solely at residue 567 existed prior to the emergence of ZM1. Since variants were selected on a morphologic basis, any 4-GU-DANA-resistant variants possessing only the residue 567 alteration may not have been morphologically distinct from WT and thus not selected for study. Identification and analysis of these putative singly mutated resistant variants could be performed, even if the variants lack identifiable phenotypes, by screening for 4-GU-DANA resistance.

The in vitro and in vivo efficacy of 4-GU-DANA against influenza virus has been attributed to the neuraminidase-in-

hibitory effect of this compound (24, 27, 40). Recent studies on 4-GU-DANA revealed not only the ability of these molecules to inhibit the neuraminidase activity and the HN receptor binding of HPF3 (9, 18) but also the inhibitory effect of 4-GU-DANA on the fusogenic function of influenza virus HA (9). Thus, interestingly and somewhat paradoxically, molecules rationally designed as inhibitors of influenza virus NA exert effects on HPF3 viral functions that do not involve neuraminidase function.

ZM1 is the first paramyxovirus variant selected with a sialic acid analog neuraminidase inhibitor. As such, there is no established evidence for the mechanisms of 4-GU-DANA escape by viruses of this family. However, data generated from the numerous influenza virus 4-GU-DANA escape variant studies suggest explanations for the resistance of HPF3 to this inhibitor (2, 3, 10–12, 20–22, 28, 34, 35).

The guanidiny group of 4-GU-DANA was predicted to make energetically favorable interactions with the side chain carboxylic acid groups of the influenza virus NA framework, or structural, residues E119 and E227 in the active-site pocket (40). Amino acid E119 is commonly mutated in influenza virus NA following in vitro selection with 4-GU-DANA (2, 3, 10–12, 34), and influenza virus escape variants possessing alterations at this residue had a reduced affinity for the inhibitor due to loss of stabilizing interactions between E119's carboxylate residue and the guanidiny group of 4-GU-DANA (3). The corresponding residue in HPF3 HN is T193, which was altered in both our C-0 and ZM1 variants. The structural similarities between influenza virus NA and paramyxovirus HN suggested that homologous residues might serve similar functional roles, specifically in the context of inhibition by 4-GU-DANA. It seems possible that HPF3 HN residue T193 provides important interactions with the inhibitor guanidiny group and that a mutation at this site could, as identified in influenza virus studies, confer resistance. Interestingly, however, the C-0 T193A alteration in HPF3 HN did not confer 4-GU-DANA resistance.

Unlike influenza virus, in which separate surface glycoproteins are responsible for the neuraminidase and receptor-binding activities, most members of the *Paramyxoviridae* family possess a dual-function HN molecule. The existence of separate sites for the receptor-binding and neuraminidase functions of the paramyxovirus HN molecule has been debated extensively. Studies of various paramyxovirus family members with mutations in different HN residues have addressed this question by attempting to ascribe functional roles to these residues; the varied results have failed to elucidate definitively whether the dual HN functions reside in the same or distinct sites. Analysis of our ZM1 variant supports the possibility of a single site capable of affecting both binding and enzymatic properties. The alteration at residue 567 conferred 4-GU-DANA resistance for both receptor binding and neuraminidase activity; the presence of a single, multifunctional site on HPF3 HN therefore appeared likely. NDV HN residue 175 corresponds to HPF3 HN 193 (the analog of influenza virus NA E119); mutation at this position resulted in alteration of both receptor recognition and neuraminidase activity and suggested the presence of a single site on HN for both functions (16, 32). A single site was also implicated in a study of bovine parainfluenza 3 in which residue 193, the HPF3 193 correlate,

affected both hemagglutinating and neuraminidase activities and thus suggested a single site (33). In contrast, mutation of the homologous residue in mumps virus HN (I181T) resulted in altered neuraminidase activity; receptor-binding activity was unchanged (42). This work suggested, by virtue of the separate effects on binding and neuraminidase activities, the presence of two sites on mumps virus HN. Several studies using monoclonal antibodies to select for Sendai virus escape variants postulated an HN with dual sites (8, 19, 29, 30, 36). Recently, Crennell et al. presented crystallographic evidence suggestive of a single, conformationally switchable site in NDV HN (6), a conclusion consistent with our findings in the ZM1 4-GU-DANA variant since one amino acid change resulted in dual-function ZM1 HN resistance.

For influenza virus, the balance of NA and HA activities is important for both the emergence of 4-GU-DANA resistance and the retention of in vivo viability. If virus binds receptor avidly, then entry will be efficient while release will be hindered, resulting in loss of viability; if receptor binding is reduced drastically, then entry of the virus is compromised, resulting in a similar loss of viability. It is the balance of these two functions that determines the functional characteristics of influenza virus, including its ability to escape inhibition by a molecule like 4-GU-DANA.

Balance of the dual functions of HN is also important for the functional characteristics of HPF3 even though the distinct biological activities of receptor binding and receptor destruction reside on a single molecule. For example, our fusogenic C-0 variant incurred a single amino acid change that altered only its receptor-binding affinity (25); another fusogenic HPF3 variant, C-28, possessed a single alteration that reduced the neuraminidase activity while sparing its receptor-binding affinity (15). However, both variants exhibit similar highly fusogenic phenotypes distinct from that of WT HPF3. Thus, it is possible to affect HN functions separately, and similar to the case for influenza virus, the balance of binding and release influences the outcome of HPF3 infection.

Although the ZM1 variant exhibited 4-GU-DANA resistance in measures of both receptor binding and neuraminidase activity, the possibility exists that HPF3 viral escape, unlike influenza virus escape, necessitates alterations in both the binding and neuraminidase activities, although this scenario is unlikely. As a hypothetical example, the isolation of HPF3 variants displaying sensitivity to the HAD-inhibiting effects of 4-GU-DANA but resistance to the neuraminidase-inhibiting effects would suggest that inhibition by 4-GU-DANA could be circumvented via alterations solely in the neuraminidase activity. However, ZM1 exhibited similar levels of resistance for both HN activities. One interpretation of this result involves alterations of a single, multifunctional site on HN that disrupt interactions with 4-GU-DANA and alter both the binding and neuraminidase activities in the presence of the inhibitor. Characterization of additional escape mutants may provide further insight into the mechanisms of 4-GU-DANA resistance. Such variants may provide additional evidence not only of the existence of a single site on HN, which has been most recently and convincingly postulated by Crennell et al. (6), but also of the inseparability of HN's receptor-binding and receptor-destroying activities as they relate to 4-GU-DANA resistance.

Influenza virus 4-GU-DANA-resistant variants have been

difficult to isolate in vitro as discussed above, and this difficulty has been reflected in the paucity of variants arising in vivo. Nevertheless, the emergence of resistant variants indicates that resistance in vivo is possible. Evaluation of these variants in animal models has been an important assessment of their viability and thus their potential impact upon introduction of 4-GU-DANA into clinical use. Studies performed with mice have yielded varied results regarding the variants' ability to replicate—with many variants being less viable than WT counterparts—and to resist inhibition by 4-GU-DANA (reviewed in reference 23). Studies using the cotton rat will be performed to assess both the viability of ZM1 and its in vivo 4-GU-DANA sensitivity. The ability of ZM1 to replicate within nasal and respiratory epithelium as well as to undergo multiple rounds of entry and release in the presence of 4-GU-DANA will be examined. These experiments will provide not only information regarding the in vivo relevance of ZM1 but also insight into the potential use of this class of antivirals in the treatment and therapy of HPF3 infection.

Although 4-GU-DANA was not a potent inhibitor of the biological activities of HPF3 in vitro, these results must be tempered with the fact that the molecule was specifically designed for inhibition of the influenza NA active site and not the HPF3 HN site(s). Further advances in the use of this class of neuraminidase inhibitors for human paramyxovirus infections may rely on the crystallographic data for NDV HN (6).

Although the work of Crennell et al. (6) presents a structural description of a nonhuman pathogen, it may nevertheless serve as a useful model for the molecular design of more specific and potent inhibitors of human pathogens as has been accomplished for influenza virus. 4-GU-DANA may not be a suitable clinical inhibitor of the paramyxovirus HN, given the high concentrations necessary for in vitro efficacy; nevertheless, development of more effective molecules within this class of inhibitors now seems imminently possible and thus promises to alter the prophylaxis and treatment of these infections.

ACKNOWLEDGMENTS

This work was supported by Public Health Service grant AI 31971 to A.M. from the National Institutes of Health.

We thank Richard Peluso for helpful discussions, and we thank Rob Fenton, Glaxo Wellcome Research and Development Ltd. (Stevenage, United Kingdom), for helpful discussions and for providing zanamivir.

REFERENCES

- Baker, A. T., J. N. Varghese, W. G. Laver, G. M. Air, and P. M. Colman. 1987. The three-dimensional structure of neuraminidase of subtype N9 from an avian influenza virus. *Proteins Struct. Funct. Genet.* **2**:111–117.
- Barnett, J. M., A. Cadman, F. M. Burrell, S. H. Madar, A. P. Lewis, M. Tisdale, and R. Bethell. 1999. In vitro selection and characterisation of influenza B/Beijing/1/87 isolates with altered susceptibility to zanamivir. *Virology* **265**:286–295.
- Blick, T. J., T. Tiong, A. Sahasrabudhe, J. N. Varghese, P. M. Colman, G. J. Hart, R. C. Bethell, and J. L. McKimm-Breschkin. 1995. Generation and characterization of an influenza virus neuraminidase variant with decreased sensitivity to the neuraminidase-specific inhibitor 4-guanidino-Neu5Ac2en. *Virology* **214**:475–484.
- Burmeister, W. P., W. H. Ruigrok, and S. Cusack. 1992. The 22 Å resolution crystal structure of influenza B neuraminidase and its complex with sialic acid. *EMBO J.* **11**:49–56.
- Colman, P. M., P. A. Hoyne, and M. C. Lawrence. 1993. Sequence and structure alignment of paramyxovirus hemagglutinin-neuraminidase with influenza virus neuraminidase. *J. Virol.* **67**:2972–2980.
- Crennell, S., T. Takimoto, A. Portner, and G. Taylor. 2000. Crystal structure of the multifunctional paramyxovirus hemagglutinin-neuraminidase. *Nat. Struct. Biol.* **7**:1068–1074.
- Durbin, A. P., S. P. Hall, J. W. Siew, S. S. Whitehead, P. L. Collins, and B. R. Murphy. 1997. Recovery of infectious human parainfluenza virus type 3 from cDNA. *Virology* **235**:323–332.
- Gorman, W. L., D. S. Gill, R. A. Scroggs, and A. Portner. 1990. The hemagglutinin-neuraminidase glycoproteins of human parainfluenza virus type 1 and Sendai virus have high structure-function similarity with limited antigenic cross-reactivity. *Virology* **175**:211–221.
- Greengard, O., N. Poltoratskaia, E. Leikina, J. Zimmerberg, and A. Moscona. 2000. The anti-influenza virus agent 4-GU-DANA (zanamivir) inhibits cell fusion mediated by human parainfluenza virus and influenza virus HA. *J. Virol.* **74**:11108–11114.
- Gubareva, L. V., R. C. Bethell, C. R. Penn, and R. G. Webster. 1996. In vitro characterization of 4-guanidino-Neu5Ac2en-resistant mutants of influenza A virus, p. 753–760. *In* L. E. Brown, A. W. Hampson, and R. G. Webster (ed.), *Options for the control of influenza III*. Elsevier, Amsterdam, The Netherlands.
- Gubareva, L. V., R. Bethell, G. J. Hart, K. G. Murti, C. R. Penn, and R. G. Webster. 1996. Characterization of mutants of influenza A virus selected with the neuraminidase inhibitor 4-guanidino-Neu5Ac2en. *J. Virol.* **70**:1818–1827.
- Gubareva, L. V., M. J. Robinson, R. C. Bethell, and R. G. Webster. 1997. Catalytic and framework mutations in the neuraminidase active site of influenza viruses that are resistant to 4-guanidino-Neu5Ac2en. *J. Virol.* **71**:3385–3390.
- Hayden, F. G., A. D. Osterhaus, J. J. Treanor, D. M. Fleming, F. Y. Aoki, K. G. Nicholson, A. M. Bohnen, H. M. Hirst, O. Keene, and K. Wightman. 1997. Efficacy and safety of the neuraminidase inhibitor zanamivir in the treatment of influenza virus infections. GG167 Influenza Study Group. *N. Engl. J. Med.* **337**:874–880.
- Hoffman, M. A., and A. K. Banerjee. 1997. An infectious clone of human parainfluenza virus type 3. *J. Virol.* **71**:4272–4277.
- Huberman, K., R. Peluso, and A. Moscona. 1995. The hemagglutinin-neuraminidase of human parainfluenza virus type 3: role of the neuraminidase in the viral life cycle. *Virology* **214**:294–300.
- Iorio, R. M., R. J. Sydall, R. L. Glickman, A. M. Riel, J. P. Sheehan, and M. A. Bratt. 1989. Identification of amino acid residues important to the neuraminidase activity of the HN glycoprotein of Newcastle disease virus. *Virology* **173**:196–204.
- Langedijk, J. P., F. J. Daus, and J. T. van Oirschot. 1997. Sequence and structure alignment of *Paramyxoviridae* attachment proteins and discovery of enzymatic activity for a morbillivirus hemagglutinin. *J. Virol.* **71**:6155–6167.
- Levin Perlman, S., M. Jordan, R. Brossmer, O. Greengard, and A. Moscona. 1999. The use of a quantitative fusion assay to evaluate HN-receptor interaction for human parainfluenza virus type 3. *Virology* **265**:57–65.
- Lyn, D., M. B. Mazanec, J. G. Nedrud, and A. Portner. 1991. Location of amino acid residues important for the structure and biological function of the hemagglutinin-neuraminidase glycoprotein of Sendai virus by analysis of escape mutants. *J. Gen. Virol.* **72**:817–824.
- McKimm-Breschkin, J. L., T. J. Blick, A. Sahasrabudhe, J. N. Varghese, R. C. Bethell, G. J. Hart, C. R. Penn, and P. M. Colman. 1996. Influenza virus variants with decreased sensitivity to 4-amino- and 4-guanidino-Neu5Ac2en, p. 726–734. *In* L. E. Brown, A. W. Hampson, and R. G. Webster (ed.), *Options for the control of influenza III*. Elsevier, Amsterdam, The Netherlands.
- McKimm-Breschkin, J. L., T. J. Blick, A. Sahasrabudhe, T. Tiong, D. Marshall, G. J. Hart, R. C. Bethell, and C. R. Penn. 1996. Generation and characterization of variants of NWS/G70C influenza virus after in vitro passage in 4-amino-Neu5Ac2en and 4-guanidino-Neu5Ac2en. *Antimicrob. Agents Chemother.* **40**:40–46.
- McKimm-Breschkin, J. L., A. Sahasrabudhe, T. J. Blick, M. McDonald, P. M. Colman, G. J. Hart, R. C. Bethell, and J. N. Varghese. 1998. Mutations in a conserved residue in the influenza virus neuraminidase active site decreases sensitivity to Neu5Ac2en-derived inhibitors. *J. Virol.* **72**:2456–2462.
- McKimm-Breschkin, J. L. 2000. Resistance of influenza viruses to neuraminidase inhibitors—a review. *Antiviral Res.* **47**:1–17.
- Meindl, P., G. Bodo, P. Palese, J. L. Schulman, and H. Tuppy. 1974. Inhibition of neuraminidase activity by derivatives of 2-deoxy-2,3-dehydro-N-acetylneuraminic acid. *Virology* **58**:457–463.
- Moscona, A., and R. W. Peluso. 1993. Relative affinity of the human parainfluenza virus 3 hemagglutinin-neuraminidase for sialic acid correlates with virus-induced fusion activity. *J. Virol.* **67**:6463–6468.
- Palese, P., and R. W. Compans. 1976. Inhibition of influenza virus replication in tissue culture by 2-deoxy-2,3-dehydro-N-trifluoroacetylneuraminic acid (FANA): mechanism of action. *J. Gen. Virol.* **33**:159–163.
- Palese, P., J. L. Schulman, G. Bodo, and P. Meindl. 1974. Inhibition of influenza and parainfluenza virus replication in tissue culture by 2-deoxy-2,3-dehydro-N-trifluoroacetylneuraminic acid (FANA). *Virology* **59**:490–498.
- Penn, C. R., J. M. Barnett, R. C. Bethell, R. Fenton, K. L. Gearing, N. Healy, and A. J. Jowett. 1996. Selection of influenza virus with reduced sensitivity in vitro to the neuraminidase inhibitor GG167 (4-guanidino-Neu5Ac2en): changes in haemagglutinin may compensate for loss of neuraminidase activ-

- ity, p. 735–740. In L. E. Brown, A. W. Hampson, and R. G. Webster (ed.), *Options for control of influenza III*. Elsevier, Amsterdam, The Netherlands.
29. **Portner, A.** 1981. The HN glycoprotein of Sendai virus: analysis of site(s) involved in hemagglutinating and neuraminidase activities. *Virology* **115**: 375–384.
 30. **Portner, A., R. A. Scroggs, and D. W. Metzger.** 1987. Distinct functions of antigenic sites of the HN glycoprotein of Sendai virus. *Virology* **158**:61–68.
 31. **Potier, M., L. Mameli, M. Belislem, L. Dallaire, and S. B. Melanxon.** 1979. Fluorimetric assay of neuraminidase with a sodium 4-methylumbelliferyl- α -D-N-acetylneuraminidase substrate. *Anal. Biochem.* **94**:287–296.
 32. **Sheehan, J., and R. Iorio.** 1992. A single amino acid substitution in the hemagglutinin-neuraminidase of Newcastle disease virus results in a protein deficient in both functions. *Virology* **189**:778–781.
 33. **Shioda, T., S. Wakao, S. Suzu, and H. Shibuta.** 1988. Differences in bovine parainfluenza 3 virus variants studied by sequencing of the genes of viral envelope proteins. *Virology* **162**:388–396.
 34. **Staschke, K. A., J. M. Colacino, A. J. Baxter, G. M. Air, A. Bansal, W. J. Hornback, J. E. Munroe, and W. G. Laver.** 1995. Molecular basis for the resistance of influenza viruses to 4-guanidino-Neu5Ac2en. *Virology* **214**: 642–646.
 35. **Tai, C. Y., P. A. Escarpe, R. W. Sidwell, M. A. Williams, W. Lew, H. Wu, C. U. Kim, and D. B. Mendel.** 1998. Characterization of human influenza virus variants selected in vitro in the presence of the neuraminidase inhibitor GS 4071. *Antimicrob. Agents Chemother.* **42**:3234–3241.
 36. **Thompson, S. D., and A. Portner.** 1987. Localization of functional sites on the hemagglutinin-neuraminidase glycoprotein of Sendai virus by sequence analysis of antigenic and temperature-sensitive mutants. *Virology* **160**:1–8.
 37. **Tulip, W. R., J. N. Varghese, A. T. Baker, and A. van Donkelaar.** 1991. Refined atomic structures of N9 subtype influenza virus neuraminidase and escape mutants. *J. Mol. Biol.* **221**:487–497.
 38. **Varghese, J. N., and P. M. Colman.** 1991. Three-dimensional structure of the neuraminidase of influenza virus A/Tokyo/3/67 at 2.2 Å resolution. *J. Mol. Biol.* **221**:473–486.
 39. **Varghese, J. N., W. G. Laver, and P. M. Colman.** 1983. Structure of the influenza virus glycoprotein antigen neuraminidase at 2.9 Å resolution. *Nature* **303**:35–40.
 40. **von Itzstein, M., W. Y. Wu, G. B. Kok, M. S. Pegg, J. C. Dyason, B. Jin, T. V. Phan, M. L. Smythe, H. F. White, S. W. Oliver, P. M. Colman, J. N. Varghese, D. M. Ryan, J. M. Woods, R. C. Bethell, V. J. Hotham, J. M. Cameron, and C. R. Penn.** 1993. Rational design of potent sialidase-based inhibitors of influenza virus replication. *Nature* **363**:418–423.
 41. **Warner, T. G., and J. S. O'Brien.** 1979. Synthesis of 2'-(4-methylumbelliferyl)- α -D-N-acetylneuraminic acid and detection of skin fibroblast neuraminidase in normal humans and in sialidosis. *Biochemistry* **18**:2783–2787.
 42. **Waxham, M. N., and J. Aronowski.** 1988. Identification of amino acids involved in the sialidase activity of the mumps virus hemagglutinin-neuraminidase protein. *Virology* **167**:226–232.